Application of Response Surface Method using Rapid Screening, Support Vector Machine, and Multiple Regression on the Acidity and Activity of Si−Al−Zr Ternary Oxide

Kohji Omata,*,† Yuichiro Yamazaki,† Yasukazu Kobayashi,† and Muneyoshi Yamada‡

Department of Applied Chemistry, Graduate School of Engineering, Tohoku University, Aoba 6-6-07, Aramaki, Aoba-ku, Sendai 980-8579, Japan, and Akita National College of Technology, Bunkyo-cho 1-1, Iijima, Akita 011-8511, Japan

Received December 16, 2009

To study the synergistic effect on the acidity and activity of Si−Al−Zr ternary oxide system, the mixture design of experiments was applied to prepare the ternary oxides by a sol−gel method, and rapid screening on dehydration of isopropanol and Friedel−Crafts reaction was conducted to determine the activities. These activities, amount of acid site determined by pyridine pulse, and specific surface area, were correlated with the oxide composition by means of support vector machine. Clear synergy among the Si−Al−Zr was observed on the acidic character and the surface area, whereas no synergy between Al−Zr was observed on the catalytic activities. Multiple regression was then conducted to find a relationship between the activities and the characters. The term of Si molar fraction in the oxide was essential for good regression, and acid strength determined by peak temperature of NH_3 desorption was related to the Si fraction. Thus, simple and rapid technique for activity test and characterization can be integrated by means of support vector machine and multiple regression, and some insights of the active site were obtained.

Introduction

Solid acids are required to play a significant role in the green chemistry of fine and specialty chemicals manufacturing process.[1] A variety of industrial processes using solid acids, such as alkylation, isomerization, cracking, and etherification, have been established, and catalysts, such as zeolites, oxides, mixed oxides, phosphates, ion-exchange resins, and clays, are industrialized.[2] Among them, mixed metal oxides provide much functionality. Whereas the acidity of binary metal oxide can be predicted by Tanabe theory,[3] prediction of those of ternary or more complex mixed oxides is not established because of their combinatorial explosion. Thus, rapid technology is potentially required to predict the synergistic effect.

To avoid the combinatorial explosion of the oxide composition, the design of experiments (DOE) has been effectively utilized. Multiple regression using polynomial equation is applied to draw response surface from the experimental results as so-called response surface method (RSM). In the field of catalyst research, however, application of the RSM was limited probably because of the complexity and nonlinearity of the catalytic phenomena.

As reviewed in the introduction of ref 4, modeling methodologies were suggested in the research field of catalysis to overcome the complexity and nonlinearity.[5−12] It was also reported that an artificial neural network, especially a radial basis function network,[13,14] was successfully applied for the regression of catalytic phenomena instead of the conventional polynomial equation. Such methodology is effective for integrating the observation[15] and the characterization.[16−20]

Recently, support vector machines (SVMs) attract much attention because of their high generalization capability. SVM was first reported in the field of solid catalysis as a classifier.[21,22] It can be used also for regression, and by SVM the inputs are mapped into a high-dimensional space in nonlinear manner and then the modified inputs are correlated linearly with the output.[23,24] These reported results show clearly the superior generalization capability of a SVM and better availability through open source program makes SVM more applicable than an artificial neural network. In the present study, SVM was used for the regression using *libsvm* library[24] through *svm* function in package e1071 of statistic language R.[25]

Considering the demands for rapid screening, a simplified procedure of an activity test will be developed in the present study. The catalytic activity test was conducted in test tubes in parallel. The first test reaction was dehydration in a pulse mode operated at 145 °C. Isopropanol dehydration on acid cite was reported in a literature.[26] The series of alumina oxides decomposed isopropanol to mainly propylene and small amount of di-isopropyl ether was observed. The activity to propylene was dependent on the amount of the acid site. The second test reaction is Friedel−Crafts reaction in batch mode at 150 °C. Benzylation of anisole was reported to proceed on Brønsted acid, whereas dibenzyl ether was formed on Lewis acid site.[27]

* To whom correspondence should be addressed. E-mail: omata@erec.che.tohoku.ac.jp.
† Tohoku University.
‡ Akita National College of Technology.

10.1021/cc900188g
Published on Web 05/20/2010

Various indicator and techniques for solid surface acid−base characterization have been proposed, such as isoelectric point by electrokinetic titration, $H_{0,max}$ by indicator dye adsorption, chemical shift by XPS, and the heat of adsorption of probe gases by calorimetry or inverse gas chromatography.[28] In addition to the gas adsorption, model reactions can be used to characterize the acidity if all the properties of the active sites is known.[29] For example, as reported recently,[30] model reaction was successfully applied as a probe of the acidity of supported catalyst. In such cases other catalyst factors such as surface area, pore structures, location of active sites and so on, are similar each other, and thus the relation between the activity and acidity is simple. So we think not only the activity and acidity but also other factors should be included in order to find the nonlinear relationship using new method such as support vector machine. From the view points of simplicity and quantitative analysis, pulse adsorption of pyridine was applied in the present study.

The integration of the simple and rapid techniques for activity test and characterization was conducted by means of SVM and multiple regression to find rapidly the synergistic effect among the ternary oxide system.

Experimental Section

Preparation of Ternary Oxides. The notation of mixed oxide is like $Si_{25}Al_{50}Zr_{25}$ when Si/Al/Zr = 25:50:25 mol %. For the effective regression of oxide composition, composition of the mixed oxide was determined by mixture design using *gen.mixture* function in AlgDesign package as

```
library(AlgDesign)
dat<−gen.mixture(5,c("Si","Al",Zr"))*100
library(vcd)
ternaryplot(dat,scale=100,main='')
```

where total 15 experiments were designed. The designed composition is illustrated in Figure 1 as a ternary plot. Red circles in the figure show the composition of the designed oxides.

Using DOE, the number of experiments can be drastically reduced. However, the 15 experiments in this case is still too many because it takes a few weeks using the conventional one-by-one method. So, a new rapid screening method is required. According to the terms of combinatorial chemistry rapid library synthesis are highly recommended in such a situation. Affinity of liquid procedure, such as a sol−gel method, is high for automated procedure of rapid library synthesis and thus the ternary Si−Al−Zr mixed oxides were prepared by a sol−gel method. Aluminum nitrate ($Al(NO_3)_3 9H_2O$), zirconyl nitrate ($Zr(NO_3)_2O\ 2H_2O$), and ethyl orthosilicate ($Si(CH_3CH_2O)_4$) for 100 mg oxide were solved in 2 mL of mixed solvent (ethanol/water = 1:1) in a test tube (ϕ15 mm, 150 mm). Ammonia water (28%, 1 mL) was then added for the gelation. After removal of the solvent at 80−110 °C, the dry gel was calcined at 550 °C for 6 h in air. The preparation of 15 kinds of oxide was conducted in parallel.

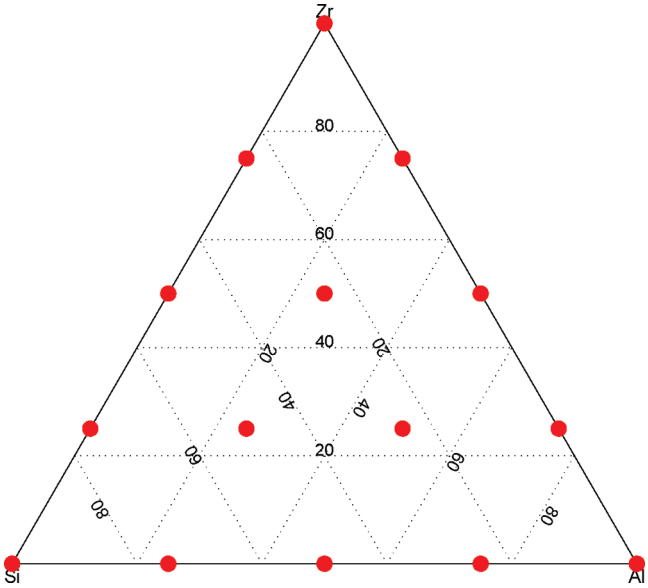

Figure 1. Ternary plot of mixture design of Si−Al−Zr ternary oxide.

Activity Test of Isopropanol Dehydration. Mixed oxide (40 mg) was sampled in a test tube (ϕ15 mm, 150 mm) and sealed by doubled-cap made of silicone. One hundred twenty seconds after isopropanol (4 μL) was dropped in the test tube at 145 °C, the test tube was cooled in water at room temperature. After it was punctured by a injection needle, the test tube was connected to a gas detector tube (Gastec, No.172 for ethylene) through another injection needle and then the gas (50 mL) was sampled. The gas detector showed high sensitivity also for detection of propylene. The 15 samples were tested in parallel intended for rapid screening. Actually, activity of 15 kinds of oxide was determined in few hours.

Activity Test of Benzylation of Anisole. The 15 kinds of mixed oxides (40 mg) were sampled in test tubes (ϕ15 mm, 150 mm) in parallel. Benzyl alcohol (0.2 g) and anisole (2.0 g) were mixed in the each tube. After 2 h reaction at 150 °C in open air, the product was analyzed by gas chromatograph (Shimadzu GC-8A, Ar carrier, Dexil 300 GC packed column at 120−190 °C) equipped with flame-ionization-detector. The main product was benzyl anisole and a small amount of dibenzyl ether was formed. Because GC analysis was time-consuming, the 15 activity tests were conducted in 2 days since the oxide preparation.

Characterization of Oxides. X-ray diffraction (Rigaku, Miniflex) was used to identify the oxide phase. The Cu Kα radiation was used as an X-ray source. The X-ray tube was operated at 30 kV and 15 mA. Diffraction intensities were recorded at 2θ from 10 to 90° at the rate of 1°/min. The observed diffraction patterns were identified by the Joint Committee on the Powder Diffraction Standards (JCPDS) card.

Specific surface area was measured by a BET method at −196 °C (Monosorb MS-19, Quantachrome) using N_2 30%/He 70 gas. The amount of acid site was determined by pyridine pulse adsorption. The mixed oxide (20 mg) was charged in flow type cell connected in the GC carrier line (GC-8A, thermal conductivity detector, He carrier, Shimadzu). After calcination for 20 min at 300 °C, 5 pyridine pulses (size = 0.5 μL) was introduced at 270 °C. After the first or second pulse, the peak area reached to steady state. The adsorbed pyridine amount was estimated from the differences. It is certain from the TPD profile of NH_3 that

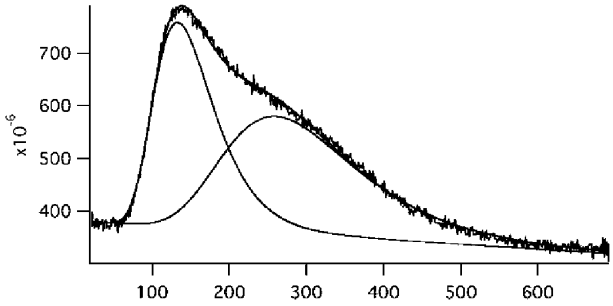

Figure 2. Curve fitting of TPD profile.

acid cites have a variety of strength. In our experiments, therefore, only strong acid site was detected by pyridine adsorption by conducting the pulse reaction at this temperature. The amount of acid sites determined by this pyridine pulse and that of strong site by NH_3-TPD was identical.

While the method is no longer rapid, a part of the mixed oxides was characterized by NH_3-TPD. The sample was pretreated in Ar flow from room temperature to 500 °C (10 K/min), held at 500 °C for 60 min. After cooling-down, NH_3 was adsorbed at room temperature for 30 min in NH_3/He (10% NH_3) flow. After removal of the vapor phase NH_3 at room temperature for 60 min in Ar flow, desorbed NH_3 profile was observed at room temperature to 700 °C (10 K/min) in Ar flow. The TPD profile was fitted to 2 peaks using an extreme function as shown in Figure 2 for chemisorbed NH_3 on weak acid site and on strong acid site, respectively. The strength of the strong acid site was determined as the highest peak temperature of the TPD profile.

Informatics. Statistic programing language R[25] was used for informatics procedure. AlgDesign package[31] was used for a design of mixture experiments with assistance of vcd package[32] for ternary plot. *svm* function in e1071 package[33] was used for the regression by support vector machine (SVM).

Result and Discussion

Phase of Mixed Oxide. X-ray diffraction patterns of the prepared oxides are illustrated in Figure 3. The numbers are same as those in Table 1. Profiles of nos. 1−4 were corrected by the profile of blank where peaks of the sample plate (aluminum metal) were recorded. Broad peaks suggest that crystalline size is small and almost part of the oxides are amorphous. Single oxide was silica (no. 1), γ-alumina (no. 5), and orthorhombic zirconia (no. 15). Peaks in no. 9 were assigned to $Al_x\,Zr_{1-x}O_y$ mixed oxide. Main peak of SiO_2 on No.1 gradually shifts to higher angle in Si−Al binary mixtures (nos. 1, 2, 3, and 4), and it suggests that silica and alumina were mixed in atomic scale. The similar mixtures were observed in Si−Zr binary system (nos. 1, 6, 10, and 13), whereas no clear trend was observed in Al−Zr binary system (nos. 5, 9, 12, 14, and 15).

Activity for Isopropanol Dehydration. Composition of the ternary oxides and the activity for isopropanol dehydration are summarized in Table 1. The relationship between the composition and the activity was analyzed by conventional multiple regression and SVM.

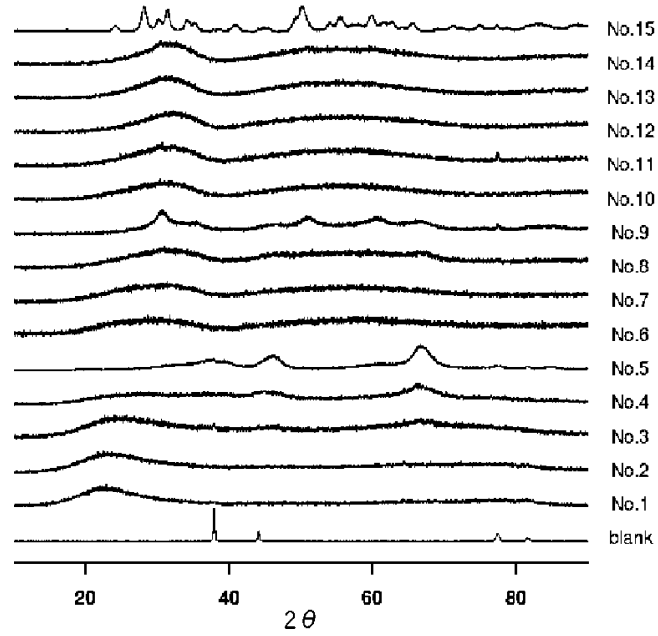

Figure 3. X-ray diffraction patterns of the designed oxides.

Prior to the analysis, libraries and experimental result were loaded.

```
library(AlgDesign)
library(e1071)
dat<−gen.mixture(5,c("Si","Al","Zr"))*100
dat$activity<−c(0,450,310,60,0,650,240,20,5,190,
 5,0,10,0,0)
```

Regression was conducted by polynomial equation in model 1. Coefficient β in eq 1 was optimized by least-squares method as follows:

```
reg<−lm(activity~.^2,dat)
summary(reg)
reg1<−step(reg)
summary(reg1)
```

$$\text{activity} = \beta_0 + \beta_1\text{Si} + \beta_2\text{Al} + \beta_3\text{Zr} + \beta_{12}\text{Si} \times \text{Al} + \beta_{13}\text{Si} \times \text{Zr} + \beta_{23}\text{Al} \times \text{Zr} \quad (1)$$

Table 1. Mixture Design of Ternary Oxide and the Activity for Isopropanol Dehydration

	oxide (mol-%)			
no.	Si	Al	Zr	propylene (ppm)
1	100	0	0	0
2	75	25	0	450
3	50	50	0	310
4	25	75	0	60
5	0	100	0	0
6	75	0	25	650
7	50	25	25	240
8	25	50	25	20
9	0	75	25	∼5
10	50	0	50	190
11	25	25	50	∼5
12	0	50	50	0
13	25	0	75	10
14	0	25	75	0
15	0	0	100	0

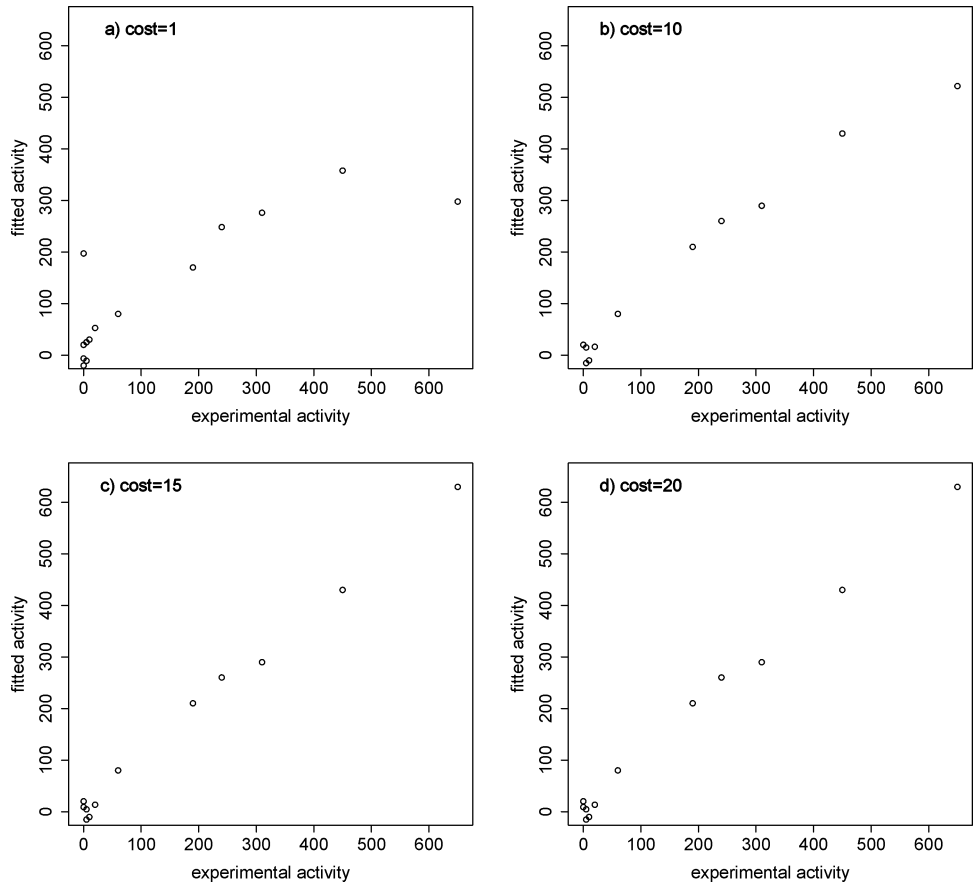

Figure 4. Change of the fitted activity in model 2: (a) cost = 1, (b) cost = 10, (c) cost = 15, and (d) cost = 20.

The result of analysis was summarized as follows:

	estimate	std error	*t* value	Pr(>|*t*|)
intercept	−59.3571	157.0029	−0.38	0.7141
Si	3.1179	2.1566	1.45	0.1822
Al	0.3357	2.1566	0.16	0.8797
Si/Al	0.0579	0.0668	0.87	0.4091
Si/Zr	0.0639	0.0668	0.96	0.3642
AL/Zr	−0.0040	0.0668	−0.06	0.9536

On the basis of the *t*-value, the statistical significance of Si, the interaction of Si × Al, and the interaction of Si × Zr are more remarkable than others. To find the influential factors, variables were selected by *step* function using AIC as an index. After trial-error steps by the function, the regression equation was simplified as expressed in eq 2. AIC of the model was improved from 160.2 to 154.59. In the final model, only Si was included in spite of the high *t*-value of Si × Al and Si × Zr terms in the initial model.

$$\text{activity} = -1.4286 + 3.9229 \times \text{Si} \qquad (2)$$

	estimate	std error	*t* value	Pr(>|*t*|)
intercept	−1.4286	61.4498	−0.02	0.9818
Si	3.9229	1.3463	2.91	0.0121

Ternary plot of activity by model 1 is illustrated in Figure 5 as a function of oxide composition. No synergy between Si−Al nor Si−Zr was observed in the figure, and as shown in eq 2, this regression failed to predict the drastic decline of the activity at high Si content resulting in the low activity of pure silica.

Other regression was conducted using SVM in models 2−4. *svm* function in e1071 package was used, and a radial basis function (RBF) was used as the kernel function. In model 2, a parameter of SVM was optimized as follows:

```
reg2<−svm(activity~.,dat, kernel="radial",cost=15)
```

Whereas parameter "gamma" was used as default (= 1/(data dimension)), the "cost" parameter (the penalty parameter of the error term) was increased from the default value 1 with checking the plot as shown in Figure 4. When no change was observed, the least value (= 15) was used for the regression. The final parameters were as follows: cost = 15, gamma = 1/3, number of support vectors = 12. They were input to reg2 variable for the prediction of activity in the following step.

In model 3, another gamma parameter (the kernel parameter of the RBFs) of SVM was also optimized simultaneously using a grid search[24] to decrease the sum of squared error between the experimental and the predicted acidity by *tune.svm* function as follows:

```
cost<−2^c(seq(−2,10,0.25))
gamma<−2^c(seq(−8,0,0.25))
model<−tune.svm(activity~., data=dat,
gamma=gamma,  cost=cost, scale=F,
tunecontrol=tune.control(sampling="fix"),
validation.x=dat[,-ncol(dat)],validation.
 y=dat[,ncol(dat)])
reg3<−model$best.model
```

The final parameters were as follows: cost = $2^{9.25}$, gamma = $2^{-7.75}$, number of support vector = 15. The parameters of the best model after the grid search were input to reg3 variable for the prediction of activity in the following step.

In model 4, leave-one-out method (in this case, 15-fold cross validation) were used in the grid search to prevent the overfitting problem as follows:

```
cost<−2^c(seq(7,11,0.25))
gamma<−2^c(seq(−14,−9,0.25))
model<−tune.svm(activity~., data=dat,
gamma=gamma,  cost=cost, scale=F,
tunecontrol=tune.control(sampling="cross",
 cross=15))
reg4<−model$best.model
```

The final parameters were as follows: cost = $2^{7.25}$, gamma = $2^{-11.00}$, number of support vector = 15.

In model 5, another kind of kernel (polynomial kernel) was employed as follows:

```
reg5<−svm(activity~., dat, kernel="polynomial",
 degree=3)
```

The default degree of the polynomial is 3.

Ternary plots of specific activity by these SVMs are also illustrated in Figure 5.

In addition to Figure 5, regression results by models 1−5 are compared for binary Si−Al oxide or Si−Zr oxide in Figure 6. Model 1 suffers from the nonlinearity of the response of activity, and model 3 clearly shows features of overfitting. The maximum activity of the binary Si−Al or Si−Zr is too low in model 4 and in model 5. As a result, the fitting by model 2 was the best among the svm models 2−5. While no significant synergy between Al and Zr was observed in this model, synergy between Si−Zr or Si−Al was clearly expressed by the regression.

Regression by SVM was suggested as the best methodology for the response surface. Regression by model 2 was used hereafter for the activity for Friedel−Crafts reaction and characterization of the oxides.

Activity for Benzylation of Anisole. The composition of mixed oxides and the activity for Friedel−Crafts reaction are summarized in Table 2. The relationship between the composition and the activity was analyzed by SVM.

The relationship between the oxide composition and the activity was correlated by SVM (model 2) as follows:

```
library(AlgDesign)
library(e1071)
dat<−gen.mixture(5,c("Si","Al","Zr"))*100
dat$activity<−c(4.5, 91.7, 67.1, 37.3, 0, 71.7,
 52.1, 22.1, 1.0, 60.1, 10.9, 0, 8.1, 0, 0)
reg_FC<−svm(activity~.,dat, kernel="radial",cost=9)
```

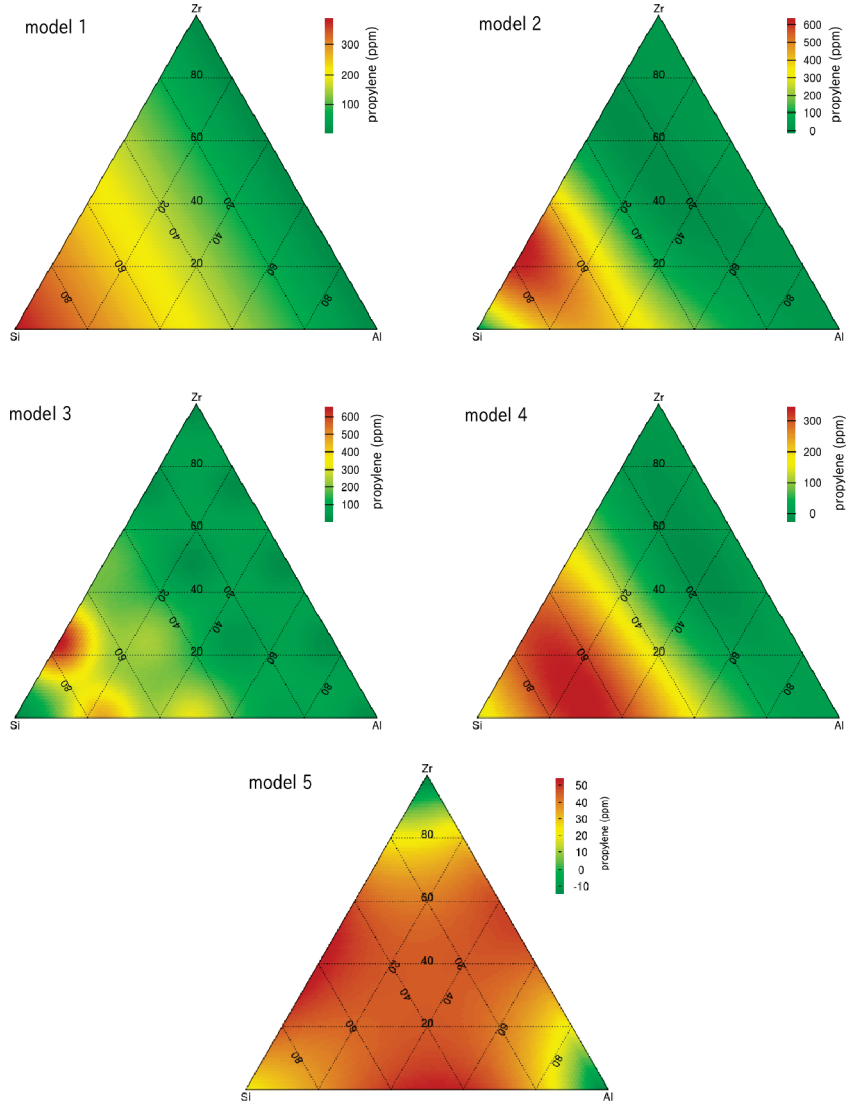

Figure 5. Response surface of activity for isopropanol dehydration by model 1−5 from upper left to down right.

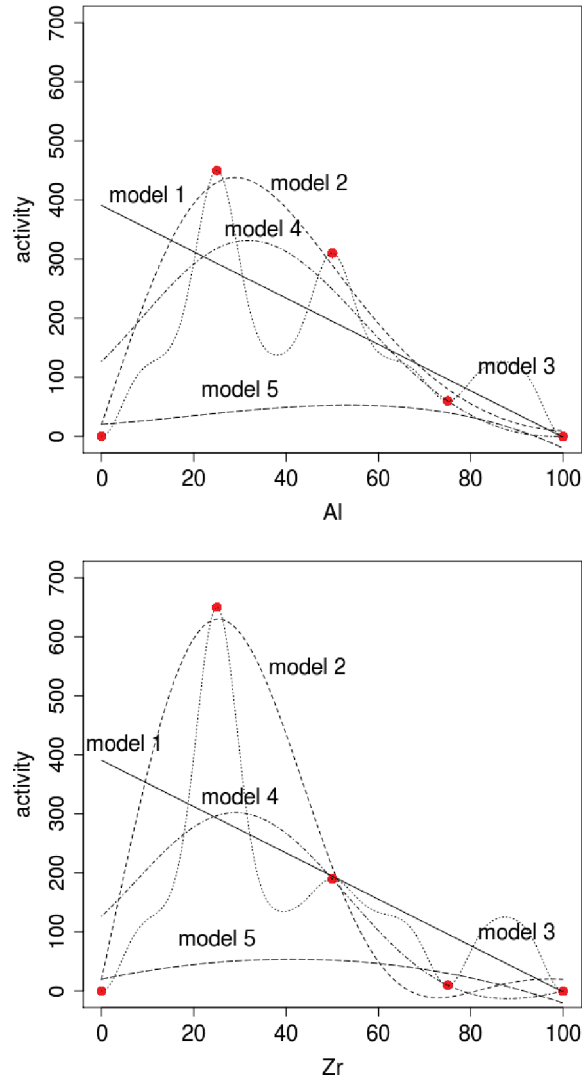

Figure 6. Comparison of regression to Si−Al or Si−Zr composition. Solid line: By multiple regression. Broken line: By SVM.

Table 2. Mixture Design of Ternary Oxide and the Activity for Benzylation of Anisole

	oxide (mol %)			benzyl anisole
no.	Si	Al	Zr	yield (%)
1	100	0	0	4.5
2	75	25	0	91.7
3	50	50	0	67.1
4	25	75	0	37.3
5	0	100	0	0
6	75	0	25	71.7
7	50	25	25	52.1
8	25	50	25	22.1
9	0	75	25	1.0
10	50	0	50	60.1
11	25	25	50	10.9
12	0	50	50	0
13	25	0	75	8.1
14	0	25	75	0
15	0	0	100	0

The parameter cost was optimized using the same method as shown in Figure 4.

The response surface of the activity is illustrated in Figure 8. Similar result was obtained with those for isopropanol dehydration, suggesting that the both reaction proceed on the same active site.

Table 3. Mixture Design of Ternary Oxide and the Oxide Character

	oxide (mol %)					
no.	Si	Al	Zr	surface area (m^2 /g)	acid amount (μmol/g)	acid density (μmol/m^2)
1	100	0	0	6	0	0.00
2	75	25	0	176	51	0.29
3	50	50	0	237	89	0.38
4	25	75	0	338	89	0.26
5	0	100	0	250	33	0.13
6	75	0	25	334	106	0.32
7	50	25	25	369	173	0.47
8	25	50	25	341	137	0.40
9	0	75	25	197	32	0.16
10	50	0	50	294	129	0.44
11	25	25	50	328	147	0.45
12	0	50	50	222	58	0.26
13	25	0	75	247	123	0.50
14	0	25	75	169	50	0.29
15	0	0	100	47	19	0.41

Characterization of the Ternary Oxides. The composition of mixed oxides and the result of oxide characterization are summarized in Table 3. The relationship between the oxide composition and the characters were correlated by SVM (model 2) using the optimized cost parameters as follows:

```
library(AlgDesign)
library(e1071)
dat<−gen.mixture(5,c("Si","Al","Zr"))*100
dat$BET<−c(6, 176, 237, 338, 250, 334, 369, 341,
 197, 294, 328, 222, 247, 169, 47)
dat$acid<−c(0, 51, 89, 89, 33, 106, 173, 137, 32,
 129, 147, 58, 123, 50, 19)
dat$density<−c(0.00, 0.29, 0.38, 0.26, 0.13,
 0.32, 0.47, 0.40, 0.16, 0.44, 0.45, 0.26, 0.50,
 0.29, 0.41)
reg_BET<−svm(BET~Si+Al+Zr, dat,
 kernel="radial", cost=10)
reg_acid<−svm(acid~Si+Al+Zr, dat,
 kernel="radial", cost=7)
reg_density<−svm(density~Si+Al+Zr, dat,
 kernel="radial", cost=5)
```

To discuss the precision of prediction by the developing model, more new test data sets should be added. One of the

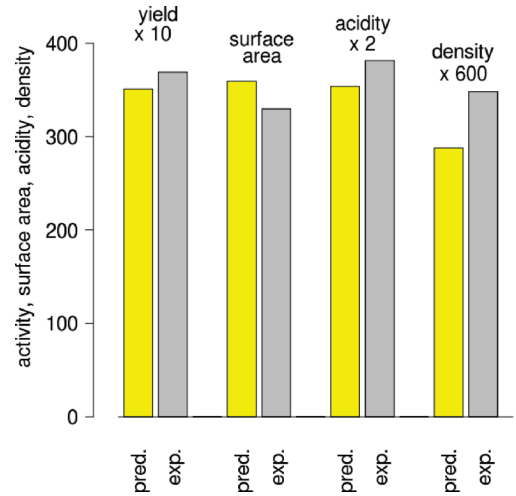

Figure 7. Verification of the prediction of Friedel−Crafts activity, specific surface area, acid amount, and acid density of $Si_{41}Al_{25}Zr_{34}$.

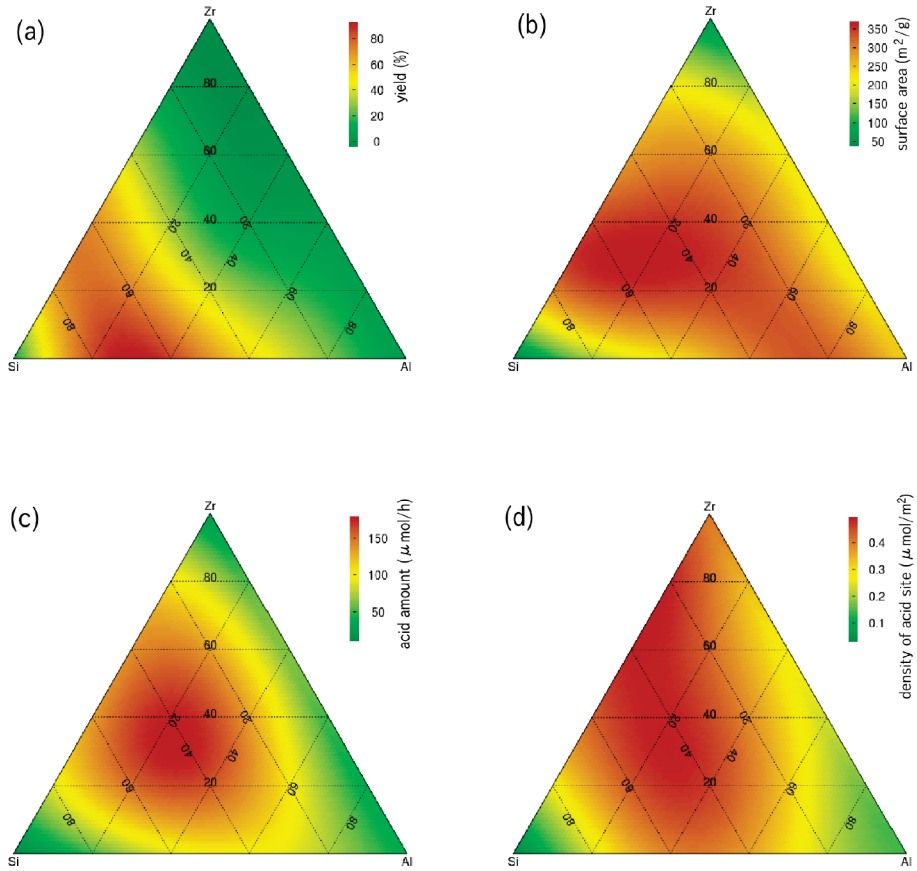

Figure 8. Response surface of activity and characters of the ternay oxides: (a) Activity for Friedel−Crafts reaction, (b) surface area, (c) amount of acid site, and (d) density of acid site from upper left to down right.

main problem of catalyst development is, however, that the preparation and activity test are time-consuming and laborious. Therefore a rapid methodology with which catalytic activity can be predicted from few experimental results are required and addition of extra test data sets is not favored for the catalyst research. Among the regression by model 1−5, it was clearly shown that SVM with RBF kernel with adequate parameters is superior for the regression of the catalysis. Thus only one extra oxide was prepared for the activity test and the characterization. From the response surface it is predicted that the maximum amount of acid site is 177 μmol/g of $Si_{41}Al_{25}Zr_{34}$. In Figure 7, the predicted characters and activity of $Si_{41}Al_{25}Zr_{34}$ were compared with those of experimentally determined. The similarity shows the predictions are precise and the regression models are valid.

The response surface of these characters are illustrated in Figure 8. Synergistic effect was clearly observed among the ternary Si−Al−Zr system in contrast to that of catalytic activity, where synergy of only Si−Al or Si−Zr was observed. The synergy for acid site was not responsible for the catalytic activity. In the each binary system, $Si_{42}Al_{58}$ or $Si_{44}Zr_{56}$ showed the highest amount of acid site. The optimum compositions are rather silica-lean from the Tanabe theory[3] where the binary oxides $Si_{60}Al_{40}$ or $Si_{65}Zr_{35}$ would show the maximum.

Multiple Regression of Characters to the Catalytic Activity. Because simple relationship between the acid amount and the catalytic activity was not observed, multiple regression using second-order polynomial equation was conducted to find correlation between them as follows:

```
reg<−lm(activity~(acidity+BET+density)^2+
 I(acidity^2) + I(BET^2)+I(density^2),exp)
tuned <− step(reg)
summary(tuned)
```

where experimental result was included in the data frame exp. As a result of variables selection by *step* function, the regression equation was

```
activity ~ acidity + BET + density +
 I(density^2) + BET:density
```

and the adjusted R-squared was as low as 0.2942. The term means the following equation where coefficient γ was optimized by *step* function.

$$\text{activity} = \gamma_0 + \gamma_1\text{acidity} + \gamma_2\text{BET} + \gamma_3\text{density} + \gamma_{33}\text{density} \times \text{density} + \gamma_{23}\text{BET} \times \text{density} \quad (3)$$

The response surface by this regression is illustrated in Figure 9. The complexity and the low R^2 suggest that the regression using only the physical properties of oxide is incomplete for good response.

Then regression using both the physical properties and catalyst composition was conducted as follows:

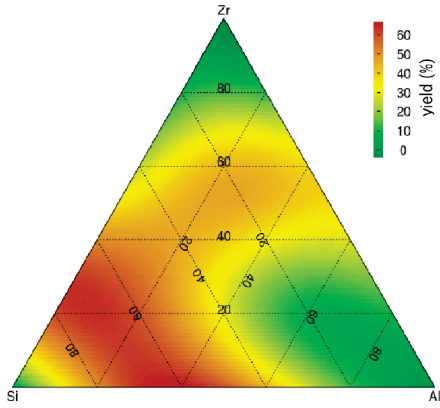

Figure 9. Response surface for the activity by regression using second-order polynomial equation of physical properties.

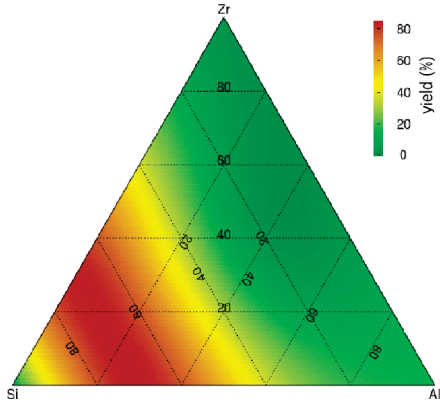

Figure 10. Response surface for the activity by regression using Si/density term.

```
reg<−lm(activity~(acidity+BET+density)+
 (acidity+BET+density):(Si+Al+Zr),exp)
tuned <− step(reg)
summary(tuned)
```

Then the best regression by which the adjusted R-squared is 0.9737 was obtained.

```
activity ~ acidity + BET + density + acidity:Al +
BET:Si + BET:Al + density:Si + density:Al
```

To simplify the equation, items with high *t* value were selected and the final regression was conducted as

```
reg<−lm(activity ~ acidity + BET +
 Si:density,exp)
tuned <− step(reg)
summary(tuned)
```

Regression with high adjusted R-squared of 0.9178 was obtained as shown below.

	estimate	std error	*t* value	Pr(>|*t*|)
intercept	3.21426	6.10980	0.526	0.60927
acidity	−0.45665	0.10312	−4.428	0.00101
BET	0.09631	0.04392	2.193	0.05070
Si/density	3.98888	0.34515	11.557	1.71×10^{7}

The high *t* value suggests statistical significance of Si/density term. The response surface by this regression is illustrated in Figure 10. The similarity of the activity in Figure 8 with that in Figure 10 confirms the validity of this regression in accordance with the high adjusted R^2. However, the origin of the importance of the Si/density term was not suggested from the experiments included in Tables 2 and 3. On the basis of the NH_3-TPD of oxides $Si_{75}Al_{25}$, $Si_{25}Al_{75}$, $Si_{75}Zr_{25}$, and $Si_{25}Zr_{75}$, the intimate relationship between the acid strength (i.e., peak temperature of TPD) and the Si:density term was suggested as shown in Figure 11. Whereas it was reported that the total amount of chemisorbed NH_3 at 80 °C was proportional to the formation rate of propylene from isopropanol dehydration on SO_4^{2-}/Al_2O_3[26] and that the amount of Brønsted acid site was proportional to the benzyl anisole yield with Nb_2O_5/Al_2O_3 catalyst,[27] the detailed analysis in the present study unveiled that the acid site strength can be also

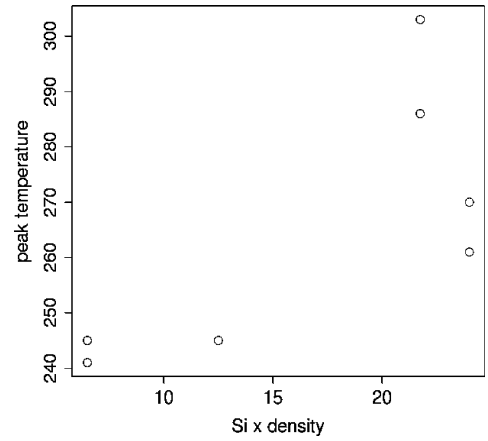

Figure 11. Relationship between the NH_3-TPD reak temperature and the density/Si term.

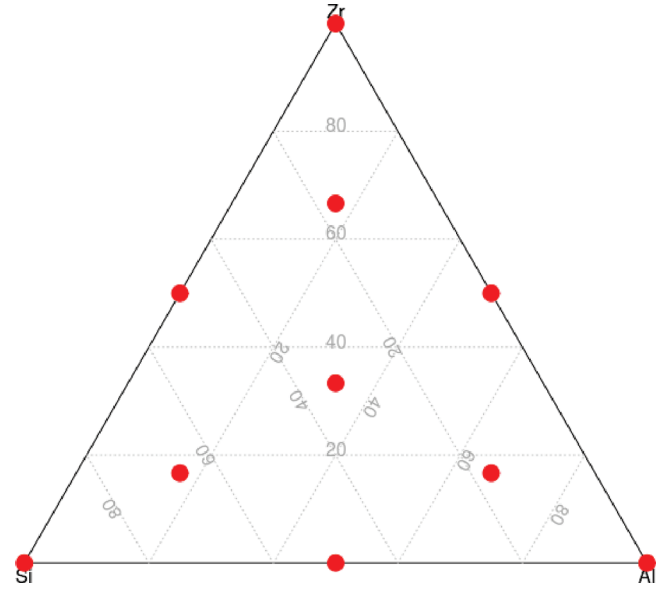

Figure 12. Augmented simplex lattice design.

Table 4. Augmented Simplex Lattice Design of Ternary Oxide and the Activity for Benzylation of Anisole

	oxide (mol %)			benzyl anisole
no.	Si	Al	Zr	yield (%)
1	100.0	0.0	0.0	4.5
2	0.0	100.0	0.0	0.0
3	0.0	0.0	100.0	0.0
4	50.0	50.0	0.0	67.1
5	0.0	50.0	50.0	0.0
6	50.0	0.0	50.0	60.1
7	66.7	16.7	16.7	83.3
8	16.7	66.7	16.7	13.7
9	16.7	16.7	66.7	2.2
10	33.3	33.3	33.3	19.8

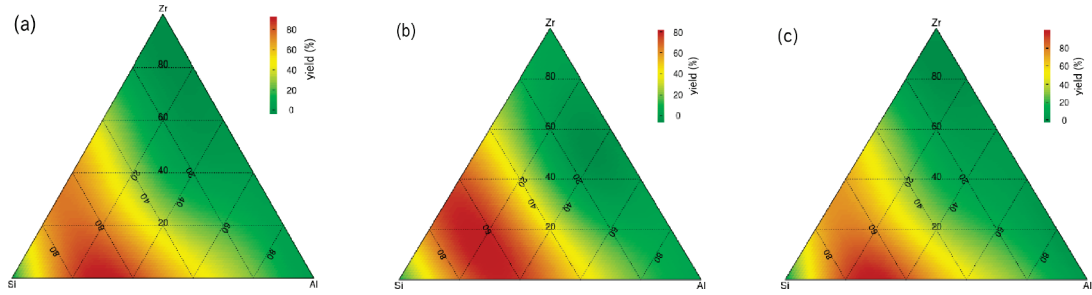

Figure 13. Comparison of experimental designs for response surface of the activity for benzylation of anisole using Si−Al−Zr oxides: (a) from simplex lattice design, (b) from augmented simplex lattice design, and (c) from the combined expepriments.

related to the catalytic activity of Si−Al−Zr ternary system.

Comparison of Experimental Design

The mixture design in Figure 1 is so-called "simplex lattice design".[34] Among the 15 experiments, 3 are for single oxide, 9 are for binary oxides, and only 3 are for ternary oxides. Because the binary oxides of Si−Al and Si−Zr are known as strong solid acid and small amount of additve such as Al or Zr to SiO_2 gives the drastic increase in their acidity,[3] assignment of many experiments to binary oxide were accordingly favorable in this study and the predictions were precise. Furthermore, attention should be paid to the performance of SVM. It can trace the rapid change of the response as shown in Figure 6 and showed better generalization ability than the conventional multiple regression. As a result, the combination of the simplex lattice design and SVM showed good performance.

However, synergy among the ternary oxide should be more included in the experimental design to find a new acidic oxide and an augmented simplex lattice design[34] (as shown in Figure 12) was compared with the simple simplex lattice design. The experimental results are summarized in Table 4.

These results were analyzed by SVM according to the procedures below and the response surfaces are illustrated in Figure 13. All the experimental results in Tables 2 and 4 were combined and used to illustrate the response surface in the right-hand side in the figure.

```
library(e1071)
Si<−c(1, 0, 0, 1/2, 0, 1/2, 2/3, 1/6, 1/6,
 1/3)*100
Al<−c(0, 1, 0, 1/2, 1/2, 0, 1/6, 2/3, 1/6,
 1/3)*100
Zr<−c(0, 0, 1, 0, 1/2, 1/2, 1/6, 1/6, 2/3,
 1/3)*100
dat<−data.frame(Si=Si,Al=Al,Zr=Zr)
activity<−c(4.5,0,0,67.1,0,60.1,83.3,
 13.7,2.2,19.8)
dat<−data.frame(Si=Si,Al=Al,Zr=Zr,
 activity=activity)
reg_FC2<−svm(activity~.,dat,
 kernel="radial",cost=15)
```

Despite the decreased number of experiments, the augmented simplex lattice design gave the response surface similar to those by the all data. However, the predicted activity is rather lower than those by simplex lattice design with 15 experiments. The activity of oxide with the highest acid site, and the highest activiy predicted by each design were compared in Table 5. The prediction by simplex lattice design

Table 5. Verification of the Predictions of the Activity for Benzylation of Anisole

		prediction by		
item	composition[a]	simplex lattice	augmented	experimental
max acid site	$Zr_{34}Al_{25}$ Si_{41}	35.1	40.9	36.9
max activity by simplex lattice	Zr_0Al_{31} Si_{69}	92.0	77.1	98.0
max activity by augmented	$Zr_{13}Al_{22}$ Si_{65}	81.5	80.6	80.2

[a] Optimum composition for the highest activity (99.3% yield) predicted by SVM based on the combined data: Zr_0Al_{30} Si_{70}.

was superior in every case. Of course it is not concluded that simplex lattice design is always superior because the activity of Si−Al binary oxide showed the highest activity by chance and synergy among the ternary or more component system usually shows better performance in many cases. A better mixture design should be developed in future.

Conclusion

The synergistic effect on the activity and acidity of Si−Al−Zr ternary oxide system was investigated. Rapid screening on dehydration of isopropanol and Friedel−Crafts reaction was conducted to determine the catalytic activities. Mixture experimental design by simplex lattice applied to the ternary mixed oxide was effective to reduce the number of the experiments. The regression of experimental results on 15 kinds of oxide were successfully conducted by support vector machine (SVM) for nonlinear response surface of the catalytic activity, specific surface area, acid amount, and acid density. Synergy among the Si−Al−Zr was observed on the acidic character and the surface area whereas no synergy between Al−Zr was observed on the catalytic activities. The discrepancy was resolved by the multiple regression to find a relationship between the activities and the characters: the term of Si molar fraction in the oxide was essential. Acid strength was suggested to be related to the importance of the Si fraction. Thus, simple and rapid technique for activity test and characterization can be integrated by means of support vector machine and multiple regression, and some insights of the active site were obtained. It is also probable that this technique can be applied to increase the amount of information in database as catalysts descriptors.[35,36] In that case, unknown interactions among the experimental results can be unveiled. If so many factors are included in the training data, the precision of the prediction of SVM should be low. The quantitative prediction by SVM should

be done using a limited number of controlled experimental conditions. In such cases, however, SVM can be utilized as classifier as an artificial neural network was used.[8] Generally SVM can provide better classification performance and would be suitable for catalyst research.

Acknowledgment. The authors acknowledge the contribution of R development team, and those of the authors and package maintainers of AlgDesign, vcd, and e1071.

References and Notes

(1) Clark, J. H. *Acc. Chem. Res.* **2002**, *35*, 791–797.
(2) Tanabe, K.; Hölderich, W. *Appl. Catal., A* **1999**, *181*, 399–434.
(3) Tanabe, K. In *General Rule of Acid of Metal Oxide (Japanese)*; Tanabe, K., Seiyama, T., Fueki, K., Eds.; Kodansha Scientific: Tokyo, 1978; Chapter III-2, p 407.
(4) Valero, S.; Argente, E.; Botti, V.; Serra, J.; Serna, P.; Moliner, M.; Corma, A. *Comput. Chem. Eng.* **2009**, *33*, 225–238.
(5) Baumes, L.; Moliner, M.; Corma, A. *QSAR Comb. Sci.* **2007**, *26*, 255.
(6) Serra, J.; Corma, A.; Valero, S.; Argente, E.; Botti, V. *QSAR Comb. Sci.* **2007**, *26*, 11–26.
(7) Farrusseng, D.; Klanner, C.; Baumes, L.; Lengliz, M.; Mirodatos, C.; Schüth, F. *QSAR Comb. Sci.* **2005**, *24*, 78–93.
(8) Baumes, L.; Farrusseng, D.; Lengliz, M.; Mirodatos, C. *QSAR Comb. Sci.* **2004**, *23*, 767–778.
(9) Holeňa, M.; Baerns, M. *Catal. Today* **2003**, *81*, 485–494.
(10) Serra, J.; Chica, A.; Corma, A. *Appl. Catal., A* **2003**, *239*, 35–42.
(11) Grubert, G.; Kondratenko, E.; Kolf, S.; Baerns, M.; van Geem, P.; Parton, R. *Catal. Today* **2003**, *81*, 337–345.
(12) Wolf, D.; Buyevskaya, O.; Baerns, M. *Appl. Catal. A* **2000**, *200*, 63–77.
(13) Omata, K.; Watanabe, Y.; Hashimoto, M.; Umegaki, T.; Yamada, M. *Ind. Eng. Chem. Res.* **2004**, *43*, 3282–3288.
(14) Umegaki, T.; Watanabe, Y.; Nukui, N.; Omata, K.; Yamada, M. *Energy Fuels* **2003**, *17*, 850–856.
(15) Serna, P.; Baumes, L.; Moliner, M.; Corma, A. *J. Catal.* **2008**, *258*, 25–34.
(16) Baumes, L.; Moliner, M.; Nicoloyannis, N.; Corma, A. *CrystEngComm* **2008**, *10*, 1321–1324.
(17) Baumes, L.; Moliner, M.; Corma, A. *Chem.—Eur. J.* **2009**, *15*, 4258–4269.
(18) Takeuchi, I.; Long, C.; Famodu, O.; Murakami, M.; Hattrick-Simpers, J.; Rubloff, G.; Stukowski, M.; Rajan, K. *Rev. Sci. Instrum.* **2005**, *76*, 062223.
(19) Gilmore, C.; Barr, G.; Paisley, J. *J. Appl. Crystallogr.* **2004**, *37*, 231–242.
(20) Barr, G.; Dong, W.; Gilmore, C. *J. Appl. Crystallogr.* **2004**, *37*, 243–252.
(21) Serra, M.; Baumes, A.; Moliner, M.; Serna, P.; Corma, A. *Comb. Chem. High Throughput Screening* **2007**, *10*, 13–24.
(22) Baumes, L.; Serra, J.; Serna, P.; Corma, A. *J. Comb. Chem* **2006**, *8*, 583–596.
(23) Nandi, S.; Badhe, Y.; Lonari, J.; Sridevi, U.; Rao, B.; Tambe, S.; Kulkarni, B. *Chem. Eng. J.* **2004**, *97*, 115–129.
(24) Fan, R.-E.; Chen, P.-H.; Lin, C.-J. *J. Mach. Learn. Res.* **2005**, *6*, 1889–1918.
(25) R Development Core Team *R: A Language and Environment for Statistical Computing*; R Foundation for Statistical Computing: Vienna, Austria, 2009; ISBN 3-900051-07-0.
(26) Gervasini, A.; Fenyvesi, J.; Auroux, A. *Catal. Lett.* **1997**, *43*, 219–228.
(27) Shishido, T.; Kitano, T.; Teramura, K.; Tanaka, T. *Catal. Lett.* **2009**, *129*, 383–386.
(28) Sun, C.; Berg, J. *Adv. Colloid Interface Sci.* **2003**, *105*, 151–175.
(29) Guisnet, M. *Stud. Surf. Sci. Catal.* **1985**, *20*, 283.
(30) Morra, G.; Farrusseng, D.; Guillon, E.; Morin, S.; Bouchy, C.; Mirodatos, C. *Top. Catal.* **2010**, *53*, 49–56.
(31) Wheeler, B. *AlgDesign*, R package version 1.0-1; 2009 (http://www.r-project.org/).
(32) Meyer, D.; Zeileis, A.; Hornik, K. *vcd: Visualizing Categorical Data*, R package version 1.2-4; 2009 (http://www.r-project.org/).
(33) Dimitriadou, E.; Hornik, K.; Leisch, F.; Meyer, D.; Weingessel, A. *e1071: Misc Functions of the Department of Statistics (e1071), TU Wien*, R package version 1.5-19; 2009 (http://www.r-project.org/).
(34) Myers, R.; Montgomery, D.; Anderson-cook, C. *Response Surface Methodology*; Wiley: New Jersey, 2009.
(35) Klanner, C.; Farrusseng, D.; Baumes, L.; Lengliz, M.; Mirodatos, C.; Schüth, F. *Angew. Chem., Int. Ed* **2004**, *43*, 5347–5349.
(36) Schüth, F.; Baumes, L.; Clerc, F.; Demuth, D.; Farrusseng, D.; Llamas-Galilea, J.; Klanner, C.; Klein, J.; Martinez-Joaristi, A.; Procelewska, J.; Saupe, M.; Schunk, S.; Schwickardi, M.; Strehlau, W.; Zech, T. *Catal. Today* **2006**, *117*, 284–290.

CC900188G